Properties of organic-inorganic hybrids

Kamminga, Machteld Elizabeth

CHAPTER 2

Experimental Strategies

In this chapter, I highlight various experimental strategies that are of central importance in all research projects carried out in this thesis. These experimental strategies include the synthesis methods, patterning techniques and X-ray diffraction data interpretation I have conducted in the following chapters. Other experimental techniques carried out by me or collaborations include magnetic measurements, electrical measurements, optical measurements, thermogravimetric analysis and theoretical analysis. These techniques are generally well-explained in literature. Moreover, these techniques are described in the experimental sections of each of chapter. Therefore, this chapter provides an overview of how I have dealt with various research questions, from an experimental perspective based on the synthesis techniques and X-ray diffraction data interpretation.

2.1 Synthesis of Single Crystals

The synthesis of various organic-inorganic hybrid materials is one of the key aspects of the research projects described in this thesis. In this section, I describe each of the synthesis methods in more detail. The methods include the synthesis of the organic precursor salts, crystal growth from slow evaporation, the layered-solution crystal-growth technique and crystal growth of air-sensitive compounds. The preferred synthesis method depends on various factors, such as the solubility and air-sensitivity of both the precursors and the end-product. The advantages and disadvantages of each method are given in this section as well.

Note that I did not use the drop-casting technique to grow single crystals. Drop-casting describes the method in which both organic and inorganic precursors are dissolved in a common solvent, and single crystals are grown by pipetting single droplets onto a substrate and heating it. As the solution evaporates quickly, crystals are formed. This process is very fast, widely used and considered a very simple way to make single crystals.[1–4] However, I have tried this a couple of times, to make $CH_3NH_3PbI_3$ and $(CH_3NH_3)_2CuCl_4$, and found that this method does not yield high-quality single crystals. In general, fast crystallization processes do not give high-quality crystals. Therefore, I have focused on more controlled and slower crystallization methods to grow high-quality

single crystals that could be used for single-crystal X-ray diffraction. While I did not use drop-casting as a technique to make single crystals, I did use it to make polycrystalline thin films. This is described in Section 2.2. The main difference here is that I drop-casted the precursor solutions onto a hydrophilic substrate, with the intention to grow a polycrystalline hybrid film.

It is important to bear in mind that single crystals are never perfect and that defects are always present. Firstly, single crystals have a finite size. While the bulk atoms mimic an infinite crystal, the surface atoms do not. Atoms on the surface do not have translational symmetry and can have dangling bonds. Secondly, crystals often have vacancies or impurity atoms that are located in the spaces between the atoms. Thirdly, defects in the form of dislocations occur in single crystals. There are two types of dislocations: screw and edge dislocations, that are often mixed in crystals. As a result, single crystals are never made of one single domain, but consist of domains which are slightly oriented from each other, formic mosaic crystals. Moreover, crystals can be twinned. Crystal twinning occurs when two or more crystals share some of the same crystal lattice points in a symmetric manner, forming an intergrowth of crystals. Crystal twinning is described in more detail in Section 2.3.4. The crystal quality becomes apparent from X-ray diffraction measurements. High-quality single crystals give rise to smaller peak widths and well-defined, round-shaped spots when measured with single-crystal X-ray diffraction. Furthermore, the refinement parameters give a clear indication of the crystal quality, as the *R*-value is based on how similar the measured intensities of symmetry-equivalent reflections are.

2.1.1 Synthesis of Organic Precursor Salts

The organic precursor salts were synthesized from an equimolar mixture of the organic component (an amine, $R-NH_2$) and HX (X = Cl, I): $R-NH_2$ (aq) + HX (aq) $\rightleftharpoons$ $R-NH_3X$ (s). A syringe was used to slowly add the acid to the organic solution. After evaporation at 70 °C, the prepared organic salt was washed three times with diethyl ether and a bright white powder was obtained. In order to dry, the salt was placed in a vacuum oven at 125 °C for 24 hours before storing.

As all wet synthesis techniques require the organic precursor salt to be dissolved, prior to forming the end product, the following reaction takes place again: $R-NH_3X$ (s) $\rightleftharpoons$ $R-NH_3^+$ (aq) + X^- (aq). I believe that this proves that preforming any organic precursor salt is not necessary, as directly adding the individual components will give the same end result: $R-NH_2$ (aq) + HX (aq) $\rightleftharpoons$ $R-NH_2$ (aq) + H^+ (aq) + X^- (aq) $\rightleftharpoons$ $R-NH_3^+$ (aq) + X^- (aq). In Chapter 8 we proved that adding the pre-made precursor salt or the individual components directly, did not influence the formation of tin- and iodine-based crystals. This means that the extra effort to make the organic precursor salt is not required.

However, there are certain situations in which it can be beneficial to make the organic precursor salt instead of using the liquid precursor. While the chemistry of both are the same, making the precursor salt allows for easy handling. Especially in the case of iodine-based salts. Iodine is relatively heavy, compared to the organic moieties. Thus, weighting

small amounts of organic precursor is significantly easier in the form of an iodide salt. Furthermore, some organic moieties do not come in pure form. Methylamine can be store-bought as 33 wt% in EtOH or 40 wt% in H_2O. Making a CH_3NH_3I salt, would avoid adding large amounts of EtOH or H_2O to the solvent.

2.1.2 Crystal Growth from Slow Evaporation

Crystal growth from slow evaporation is a relatively easy synthesis technique that is applicable to the growth of various organic-inorganic hybrids.[5,6] The basic principle behind this technique is that both organic and inorganic precursors are dissolved in a common solvent. Note that, as stated in Section 2.1.1, it does not matter if the organic precursor is added in the form of a (pre-made) halide salt or as the liquid precursor and a stoichiometric amount of HX (X = Cl, I). After dissolving, the reaction mixtures are left to slowly evaporate in an oven. Evaporation of the solvent saturates the reaction mixture until single crystals form.

The general advantage of this technique is that it is a relatively easy way to grow high-quality single crystals. Moreover, it is applicable to a large set of organic-inorganic hybrid materials, as the main requirement is that both organic and inorganic moieties should be soluble in a common solvent. As the organic precursors are generally soluble in almost all solvents, the limiting step here is the solubility of the inorganic precursor. Therefore, I have mainly used this technique to grow hybrids that are based on $MnCl_2$ (Chapter 6) or $CuCl_2$ (Chapter 9). Both $MnCl_2$ and $CuCl_2$ dissolve in EtOH and H_2O, that evaporate easily.

A disadvantage of crystal growth from slow evaporation is that, as the name suggests, the process can be quite slow. It can take several weeks or even months to grow crystals. While I find that very fast synthesis techniques, *e.g.* drop-casting, generally do not yield high-quality single crystals, it does not mean that waiting times are required to grow nice crystals. However, the main disadvantage of this technique is that it is not suitable for inorganic precursors that have a poor solubility, such as PbI_2 and BiI_3. Both compounds are hard to bring into solution. Dimethylformamide (DMF) and HI (57 wt% in H_2O) work quite well, but these solvents have boiling points of 153 °C and 127 °C, respectively, which is not as convenient as EtOH. Therefore, I have used an alternative synthesis technique (see Section 2.1.3) to grow single crystals of hybrids containing PbI_2 and BiI_3.

2.1.3 Layered-Solution Crystal-Growth Technique

The layered-solution crystal-growth technique was first described by D. Mitzi.[7] He reported the growth of high-quality single crystals of $(C_6H_5C_2H_4NH_3)_2PbCl_4$ at room temperature. In his procedure, he dissolved $PbCl_2$ in concentrated aqueous HCl, placed a less dense layer of methanol on top, and added a stoichiometric ratio of $C_6H_5C_2H_4NH_2$ (relative to the $PbCl_2$) to the top of the column. As slow diffusion takes place at the interface between the layers, high-quality single crystals of $(C_6H_5C_2H_4NH_3)_2PbCl_4$ were obtained. The crystals were isolated after approximately one year.[7]

Here, I modified the layered-solution crystal-growth technique to fit my organic-inorganic hybrid compounds. A detailed explanation of the procedure is described below. The organic molecules and metal halides were dissolved in separate solutions with large density differences. As a result, a sharp interface is formed when the two components are combined. Single crystals grow due to slow diffusion at the interface. The inorganic components, PbI_2 or BiI_3, were dissolved in concentrated (57 wt%) aqueous HI, creating a light-yellow or orange solution, respectively. This lead or bismuth iodide/HI mixture was poured into glass test tube (a standard size of 18 x 150 mm). A syringe with needle was used to make sure that the mixture is placed at the bottom of the tube, without touching the sides of the glass tube. Absolute methanol was carefully placed on top of the mixture, with another syringe and needle, without mixing both solutions. A sharp interface between the two layers was formed due to the vast difference in densities (0.791 g/mL and 1.701 g/mL for MeOH and the concentrated aqueous HI, respectively). The organic solutions were added in great excess by gently adding 15 droplets, using a glass pipette, on top of the MeOH layer. The test tubes were covered with aluminum foil and kept in the fume hood under ambient conditions. Crystals started to form at the interface and collected at the bottom of the tube, with a time ranging from a few days to a week. The crystals were obtained by washing them three times with diethyl ether, after carefully pouring the content of the test tubes through a filter. Besides being a colorless solvent with a very low vapor pressure, the crystals do not dissolve in diethyl ether. This makes diethyl ether an excellent solvent for washing the crystals. After drying under ambient conditions, all crystals were stored in a dry box.

The major advantage of the layered-solution crystal-growth technique is that high-quality single crystals can be synthesized at room temperature, within several days. Note that it took approximately one year to grow$PbCl_2$-based hybrids,[7] while the PbI_2- and BiI_3-based hybrids studied here grow within one week of time. A drawback is that the crystals tend to be small in size, and that the method cannot be applied universally, *i.e.* not all organic-inorganic compounds grow with this method. In general, this method is applicable for materials that are insoluble in many organic solvents, such as PbI_2 and BiI_3. For compounds that tend to dissolve in water and ethanol, such as $CuCl_2$ and $MnCl_2$, this method is not applicable as their hybrid forms tend to dissolve in water and ethanol as well. For these materials, growth from slow evaporation, as described in Section 2.1.2, is the most suitable method.

2.1.4 Crystal Growth of Air-Sensitive Compounds

The previously described synthesis methods are not suitable for compounds that oxidize easily, such as tin. Therefore, I have synthesized air-sensitive compounds in a closed system, under argon. The method used here, is directly based on the method described by the Kanatzidis group.[8] Here, a three-way round-bottom flask was used, where one way was used as argon inlet, one as outlet, connected to a gas bubbler, and one as entrance for the precursors. Firstly, HI and H_3PO_2 where added to the flask and degassed by bubbling argon for several minutes. The mixture was kept under argon atmosphere throughout the experiment. Secondly, SnI_2 was added from the glovebox to the acids, and left under

continuous stirring at 120 °C, using an oil bath, until fully dissolved. A clear, yellow solution was obtained. A stochiometric volume of the pre-made organic precursor salt or the organic precursor solution was added to the hot mixture, and dissolved immediately. The mixture was left under continuous stirring for several hours, until the solution has lost roughly half its original volume. As a result, a highly concentrated solution was obtained. Subsequently, the heater was switched off, and the stirring was discontinued, in order to cool down to room temperature at a rate of approximately 20 °C/h. Upon cooling, several small crystals form at the bottom of the flask. Once completed, the crystals were extracted, by washing them with toluene and stored in a nitrogen-filled glove box.

2.2 Patterning Microstructures

To pattern microstructures of organic-inorganic hybrids, I used soft lithography techniques.[9] Soft lithography is an easy and cost-effective way to make micropatterns. Note that this method is very different from the methods described in previous sections, as it is based on growing polycrystalline structures, instead of single crystals. The procedure I used is described below.

A variety of 5 x 5 mm^2 PDMS (polydimethylsiloxane) stamps were fabricated by curing a silicone elastomer and its curing agent in a 10:1 weight ratio on prepatterned Si masters. These Si masters contain line patterns with a width ranging between 1 and 80 μm and a height of 8 μm. The Si masters were cleaned with snowjet, 30 minutes of oxygen plasma cleaning, and silanized before pouring the PDMS. 10 μL of trichloro(1*H*,1*H*,2*H*,2*H*-perfluorooctyl)silane was added to a desiccator containing the Si masters, in an argon-filled glove box. Once brought under vacuum, silanization took place over night and the Si masters were stored thereafter. The elastomer was degassed to remove all air bubbles, cured at 40 °C over night, and then peeled gently from the master. The obtained PDMS stamps were soaked in ethanol for 6 days, dried on a hot plate at 50 °C for 1 h and stored in a closed box.

The patterning was performed on glass substrates by two different techniques: imprint lithography and MIMIC (micromolding in capillaries) technology. First, the glass substrates were cleaned with 2-propanol and 15 minutes of oxygen plasma cleaning, to make the surface polar. For imprint lithography, 50 μL of the precursor solution was deposited onto the clean glass substrate, prior to bringing the PDMS stamp in contact by slowly pressing the PDMS stamp into the precursor solution (*i.e.* imprinting). A self-built micromolding machine was used for perfect alignment of the stamp with the substrate and applying a pressure in a controlled manner. Here, a pressure of around 0.5 bar was applied. The stamps and substrates were cured for 2 h at 80 °C. After carefully removing the stamps, the patterns were stored. For MIMIC technology, the PDMS stamp was placed directly in conformal contact with the clean substrates, with an applied pressure of around 0.5 bar. As a result, channels of the stamp formed capillaries with the substrate. Thereafter, the precursor solution was deposited at one end of the channel-shaped stamps, and spontaneously filled the channels by capillary force. The stamps and substrates were cured for 2 h at 80 °C. After carefully removing the stamps, the patterns were stored.

2.3 X-Ray Diffraction

Structure determination by X-ray diffraction (XRD) plays a major role in all research carried out in this thesis. As stated in Chapter 1, the understanding of structure-property relations in organic-inorganic hybrid materials is of central importance. In this section, I highlight some of the key aspects of XRD that I have taken into consideration when solving the crystal structures. At first, I provide an overview of strategies I have used in single-crystal diffraction data collection and refinement. Secondly, I describe how powder XRD can be used as a powerful complementary method. Thereafter, I describe the strategies I have used when dealing with non-standard space group settings and crystal twinning.

2.3.1 Single-Crystal X-Ray Diffraction Data Collection and Refinement

Besides performing single-crystal XRD measurements on multiple crystals, to determine and confirm the true structure, there are several other aspects of single-crystal XRD data collection and refinement that I took into consideration. This is outlined below.

When the unit cell and space group of the crystal are unknown, in my opinion it is wise to collect data over the full limiting sphere. Generally, a short test scan over 24 frames of data is performed. This allows the quality of the single crystal to be confirmed, and also provides an initial estimate of the Bravais lattice. The subsequent full data collection strategy is often based on this initial estimate. For example, when a primitive hexagonal cell is proposed, only one third of a sphere is generally measured. However, I found that not measuring complete spheres of data can lead to incorrect determination of the Bravais lattice after measuring. The assumption of a tetragonal lattice before measuring, and hence measuring only a quarter of a sphere, is most likely to limit solutions to tetragonal symmetry after data collections. Furthermore, the advantage of measuring the full Ewald sphere is that complete precession images can be made afterwards. Precession images provide valuable information on systematic absences and are therefore of importance to determine the correct space group. Thus, when the compound is fully unknown, I think that collecting a full data set is the best option. Furthermore, I think it is important to redetermine the unit cell, including a much larger set of frames than the initial 24 frames made before measuring. This will give a much more likely unit cell, than before measuring, required for integrating the intensities of the reflections. Another possibiliy here is to use CELL_NOW,[10] input a large set of reflections and let the software freely run to determine a proper unit cell. While CELL_NOW is often used to determine crystal twins, see Section 2.3.4, it can also be used to determine the unit cell. This sometimes gives an alternative cell that suits the data better.

With respect to integrating the reflections, I always refined in triclinic settings. No matter how obviously the axes and angles seem to point in the direction of a particular Bravais lattice, integration in the triclinic settings prevents any reflection being omitted. This is especially important when non-primitive cells are suggested. For example, when the data are integrated in a C-centered orthorhombic cell, even if this is not the true Bravais

lattice, all reflections that are not allowed by C-centering (*hkl*: $h+k=2n$) are omitted from the dataset. Consequently, determining the space group after integration will always point in the direction of a C-centered cell, which may thus seem correct even if this is not the case. The assumption of C-centering based on only the first 24 frames, as described above, is risky. Therefore, I always integrated in triclinic settings. Once the correct space group is found, it is possible to reintegrate the data in the relevant Bravais lattice, if different to the initial assumption. Although this strategy can improve the fit parameters, a more important consideration is that it prevents the structure solution from proceeding in the wrong direction based on preliminary data.

Sometimes I found it useful to do an initial refinement in *P*1. This does not put any constraints on your data, as no atoms are related to each other by symmetry. Therefore, it can become apparent what bonding patterns your crystal has, without forcing the atoms in a certain position by symmetry. This initial refinement can show the connectivity and coordination numbers of each atom in your crystal in an unbiased way.

I always found it important to consider the possibility of crystal twinning. Therefore, I always tried refinement of an inversion twin in non-centrosymmetric space groups. Moreover, it is important to keep in mind that twinning can have a major influence on the precession images. This means that it is possible to find reflections that appear to be not allowed, while they can be allowed in another twin domain. The same holds for the E-value statistics. The E-values are normalized structure factors (the square-roots of the intensities), scaled in such a way that the mean values of E^2 equals 1. For centrosymmetric structures, there are more particularly strong and weak E-values than for non-centrosymmetric structures. The software calculates the mean value of $|E^2-1|$. Values of 0.736 for non-centrosymmetric structures and 0.968 for centrosymmetric structures are expected. However, this is only an indication and no proof. Especially in the presence of twinning, these statistics are very unreliable. Thus, I generally tried both centrosymmetric and non-centrosymmetric space groups and chose the better solution for subsequent structure refinement. More about crystal twinning is given in Section 2.3.4

When studying phase transitions and the corresponding structural changes, such as described in Chapter 5 and Chapter 6, I found it important to use the same crystal over the entire temperature range. Obviously, the entire temperature range should be measured several times, but the use of the same crystal to collect data at each temperature allows for a direct one-to-one mapping of structural changes.

2.3.2 Powder X-ray Diffraction as a Complementary Method

A large part of this thesis focuses on single-crystal XRD to determine crystal structures. However, I have used powder XRD as well. While powder XRD can also be used to determine full crystal structures, I do not think that it is the most suitable technique to determine the full crystal structure of new and complicated compounds. This is especially the case when high-quality single crystals are available. Therefore, I have only used it as a complementary method.

Powder and single-crystal XRD are different techniques as they are based on different instrumental schemes. In single-crystal XRD, the crystal rotates in the X-ray beam, while

multiple images are recorded by an area X-ray detector. The geometry of the setup and detector ensures that a discrete function of the intensities of the signal is recorded as a function of diffraction angle. As a result, each reflection is measured individually and the intensity of the spots is related to a function of the Miller indices *hkl*. Thus, single-crystal XRD provides a direct mapping of integrated intensities. The advantage of this is that most single-crystal software programs can carry out so-called Laue checks to deduce the correct Laue class for the crystal, necessary to determine the space group. The main limitation of single-crystal XRD is that while the technique is optimized for determining integrated intensities, the esd's (estimated standard deviations) on the lattice parameters are relatively large. This makes it hard to observe small orthorhombic or monoclinic distortions.

Powder XRD on the other hand, is a technique based on converging beam optics. Operating in Bragg-Bretano geometry, powder XRD produces a one-dimensional projection of the reciprocal space. The main strength of powder XRD is that this geometry is optimized for angular resolution, by measuring the intensities as a function of diffraction angle in a continuous fashion. Thus, powder XRD is the optimal technique to accurately measure unit cell parameters. However, the disadvantage of powder XRD is that it hard to distinguish Laue classes as all symmetry-equivalent reflections have the same *d*-spacing. Consequently, individual intensities cannot be measured. This is mainly a problem for the higher-symmetry crystal systems, since tetragonal, trigonal, hexagonal and cubic systems all possess more than one Laue class. Therefore, it is nearly impossible to determine the correct space group with powder XRD. Thus, I have mainly used single-crystal XRD to determine full crystal structures with corresponding space groups and I have used the angular resolution of powder XRD to determine small distortions in the unit cell parameters. Furthermore, I have used powder XRD as a complementary method for other reasons as well, as listed below.

With single-crystal XRD only one crystal can be measured at the time. This does not say anything about the phase-purity of the entire batch of crystals. Therefore, I have used powder XRD to confirm that all crystals have the same structure. This is described in Chapter 3. Therefore, powder XRD can act as an extra test, complementary to single-crystal XRD.

All micropatterns that I made in this thesis are characterized with the powder XRD setup. As the microstructures are all polycrystalline, this is an obvious choice. However, I have used single-crystal XRD to determine the crystal structure of a single crystal and used this data to fit the XRD profiles. This proved the formation of the expected phase. In fact, here I have used single-crystal XRD as a complementary method to powder XRD.

2.3.3 The Use of Non-Standard Space Group Settings

There are several conventions when it comes to defining Bravais lattices and space groups. For example, the *b*-axis is taken as the unique axis in a monoclinic cell. Moreover, β is defined as the monoclinic angle. The same holds for the unique *c*-axis in hexagonal cells, as well as $\gamma = 120°$ in hexagonal settings. However, here I show that it can be very useful to use non-standard space group settings. The main reason why I used non-

standard settings in this thesis, is because I have studied various phase-transitions. It is convenient to keep all axes the same during a phase transition. For example, when we have a phase transition from a polar phase to another polar phase, it is convenient when the polar axis remains the same throughout the description. Chapter 6, is a good example of this. However, when considering non-standard space group settings, it is important to bear in mind that not every symmetry element is described by the short space group symbol. To illustrate this, I provide an example below.

This example is obtained with help from the *Hypertext Book of Crystallographic Space Group Diagrams and Tables*, and a discussion with its author, Dr. J. K. Cockcroft.[11] Consider a unit cell with a *C*-centered lattice. Irrespective of the crystal system, the reflection condition for *C*-centering is $h+k=2n$. However, this condition automatically implies the following sub-conditions: $0kl$: $k=2n$, $h0l$: $h=2n$, $hk0$: $h+k=2n$, $h00$: $h=2n$, and $0k0$: $k=2n$. Some of these reflection conditions are the same as those described by screw axes and glide planes. If we now consider to have the space group *Cmca*, and look at the *a*-glide perpendicular to the *c*-axis, we obtain the additional reflection condition $hk0$: $h=2n$. However, due to the reflection condition $hk0$: $h+k=2n$, as induced by the *C*-centering, we also imply $hk0$: $k=2n$, which resembles the reflection condition for a *b*-glide perpendicular to the *c*-axis. Thus, instead of *Cmca*, we could have also used the non-standard *Ccmb* space group, to describe the same set of reflection conditions. In order to overcome the misleading use of either the *a*- or *b*-glide, while technically both are accounted for, De Wolff *et al.* introduced the use of an *e*-glide.[12] The idea behind this is that the letter *e* covers certain glide planes that did not have a unique symbol, such as the glide plane described above. This one can be referred to as 'either *a* or *b*'. As a result, they introduced the use of *e* in the Hermann-Mauguin symbol of five different space groups: *Abm*2 became *Aem*2 (No. 39), *Aba*2 became *Aea*2 (No. 41), *Cmca* became *Cmce* (No. 64), *Cmma* became *Cmme* (No. 67), and *Ccca* became *Ccce* (No 68.).[12] The advantage of using the symbol *e*, is that *e* is a neutral symbol, while *a* and *b* are not. Therefore, the symbol does not change upon axis permutation. For example, when we change the axes of a given unit cell from (x,y,z) to (y,z,x), *Cmca* becomes *Bbcm*: the lattice becomes *B*-centered, the mirror-plane perpendicular to the *a*-axis becomes a mirror-plane perpendicular to the *c*-axis, the *c*-glide perpendicular to the *b*-axis becomes a *b*-glide perpendicular to the *a*-axis and the *a*-glide perpendicular to the *c*-axis becomes a *c*-glide perpendicular to the *b*-axis. However, *Bbam* has the same reflection conditions as *Bbcm* and *Bbam* will be chosen over *Bbcm* as the convention is to give priority to symmetry elements of the highest type (for planes: *m* before a,b,c before *n*) and *a* before *b* before *c*. This gives rise to confusion, while the use of the *e*-glide would simply give a transformation from *Cmce* to *Bbem*, where *e* now describes either *a* or *c*.

2.3.4 Dealing with Crystal Twinning

Crystal twinning occurs when two or more intergrown crystals are formed in a symmetrical manner, by sharing some of the same crystal lattice points. As a result, a twinned crystal is defined as an aggregate in which different domains are joined together according to a specific symmetry operation: a twin law.[13] Crystal twinning can occur

when the crystals are grown under certain experimental conditions (such as temperature, pressure and stress), leading to intergrowth of different domains.

Each twin domain is responsible for its own diffraction pattern. Therefore, the diffraction pattern obtained from data collection of a single crystal is a superposition of all diffraction patterns of the twin fractions. These individual diffraction patterns are related to each other by a twin law and weighting fractions. The twin law can consist of reflection, inversion and rotation, and can be expressed as a matrix that transforms the *hkl* indices of one species into the other. The weighting fractions correspond to the quantities of the particular twin domains present in the crystal. In terms of their diffraction patterns, twinned crystals fall into two categories: the twin domains share *all* reflections or they only share *certain* reflections. When the diffraction patterns fully overlap, the crystal lattice belongs to a higher point group than the crystal lattice itself. When only certain zones of the reflections overlap, the twin law usually represents a symmetry operation that belongs to a higher symmetry supercell.[13] As twinning is not an uncommon effect in crystallography, it is important to be able to recognize the presence of twinning, to decipher the corresponding twin law and to refine the full structure properly. These are the main points of this section.

Classified by Friedel, there are four different types of twinning.[14] As stated above, after application of the twin law, the crystal lattice does overlap with the original lattice or does not. In case it does overlap, twinning can occur by merohedry, pseudo-merohedy and reticular pseudo-merohedry. When they do not overlap, twinning occurs by non-merohedry. Here I provide an extensive list and detailed overview of each of these types of twinning. As I have used SHELX97 to refine all structures, its manual is used as a reference as well.[15]

Twinning by Merohedry

Twinning by merohedry occurs when a compound crystallizes in a unit cell with a higher point group than the corresponding space group. The easiest form can occur in non-centrosymmetric space groups and is called racemic twinning. Despite the fact that the space group is non-centrosymmetric, by definition, each lattice has inversion symmetry. Thus, this would give rise to enantiomorphic domains. Here, the twin law between twin fraction 1 (h_1,k_1,l_1) and twin fraction 2 (h_2,k_2,l_2) is given by the inversion matrix.

$$\begin{bmatrix} h_2 \\ k_2 \\ l_2 \end{bmatrix} = \begin{bmatrix} -1 & 0 & 0 \\ 0 & -1 & 0 \\ 0 & 0 & -1 \end{bmatrix} \begin{bmatrix} h_1 \\ k_1 \\ l_1 \end{bmatrix}$$

The need for a racemic twin is usually indicated by the Flack parameter x, defined as follows:[16]

$$|F(h,k,l,x)|^2 = (1-x)\,|F(h,k,l)|^2 + x|F(-h,-k,-l|^2 \tag{2.1}$$

In SHELX97,[15] refinement of the structure is carried out by full-matrix least-squares techniques. Here, $F(h,k,l,x)$ is the scaled observed structure factor and $F(h,k,l)$ and $F(-h,-k,-l)$ are the calculated structure factors of the regular and inverted *hkl*, respectively. The idea here is that the structure is refined with a racemic (*i.e.* inversion)

twin, where x corresponds to the twin ratio. As a result, x can take up any value between 0 and 1. When the atomic coordinate set and the crystal have the same chirality or polarity, x takes the value of 0, whereas when they are opposed x becomes 1. If the value is near 0.5, the crystal is most likely twinned by the inversion matrix. Note that for a centrosymmetric crystal x is undefined.

The other possibility occurs in lower-symmetry trigonal, tetragonal, hexagonal and cubic crystal systems. Due to twinning, the lower symmetry Laue groups look like the corresponding higher symmetry Laue group. As an example, we consider the true and low-symmetry tetragonal space group $P4_1$ (Laue group $4/m$) and a twin described by a 2-fold axis around [110], *i.e.* a mirror perpendicular to a and b. As a result, the diffraction pattern will make the Laue group *look like* the higher-symmetry tetragonal Laue group $4/mmm$, when x equals 0.5. The twin matrix is given below. The same matrix also applies to low-symmetry trigonal, hexagonal and cubic crystal structures, producing diffraction patterns with apparent $\bar{3}m1$, $6/mmm$ and $m\bar{3}m$ symmetry, respectively, when the domain scale factor x equals 0.5. These point groups that describe the overall symmetry of the lattice are called holohedral point groups.[13] Subgroups of holohedral point groups are referred to as merohedral point groups. For example, the hexagonal $6/m$ merohedral point group is a subgroup of the hexagonal $6/mmm$ holohedral point group.

$$\begin{bmatrix} h_2 \\ k_2 \\ l_2 \end{bmatrix} = \begin{bmatrix} 0 & 1 & 0 \\ 1 & 0 & 0 \\ 0 & 0 & -1 \end{bmatrix} \begin{bmatrix} h_1 \\ k_1 \\ l_1 \end{bmatrix}$$

Twinning by Pseudo-Merohedry

Twinning by pseudo-merohedry resembles twins that may occur in crystals that have cell dimensions that mimic those of a higher-symmetry crystal system. Note that this is different from twinning by merohedry, where a low-symmetry structure has a high-symmetry lattice, that belongs to the *same* crystal system. For twinning by pseudo-merohedry, the lattice can 'accidentally' belong to a *different* (higher-symmetry) crystal system. This type of twinning is quite common. The easiest example to illustrate this is when we consider a crystal, which has a unit cell described by $a = b = c$ and $\alpha = \beta = \gamma = 90°$. While this is a mathematical description of a cube, this does *not* imply that the crystal should have cubic *symmetry*, *i.e.* a 3-fold rotation axis perpendicular to the (111) plane.[17] Other twins by pseudo-merohedry are described in more detail below.

Orthorhombic unit cells with a and b approximately equal in length may emulate tetragonal. Orthorhombic space groups do not exhibit a 4-fold rotation axis around c, while tetragonal space groups do.[17] Thus, when a and b are approximately equal in length, twin fractions that are related by a rotation of 90° around c is possible. As a result, the two twin fractions in the orthorhombic cell mimic the 4-fold rotation axis that would have been present in tetragonal symmetry. The matrix below describes how twin fraction 2 (h_2, k_2, l_2) is related to twin fraction 1 (h_1, k_1, l_1).

$$\begin{bmatrix} h_2 \\ k_2 \\ l_2 \end{bmatrix} = \begin{bmatrix} 0 & 1 & 0 \\ 1 & 0 & 0 \\ 0 & 0 & -1 \end{bmatrix} \begin{bmatrix} h_1 \\ k_1 \\ l_1 \end{bmatrix}$$

On the other hand, monoclinic unit cells with $\beta \approx 90°$ may emulate orthorhombic. This is what I encountered in Chapter 5. To decipher the possible twin law, we use the argument described by Parkin.[18] At first, we consider the differences between monoclinic and orthorhombic symmetry. By definition,[17] monoclinic symmetry is described by any of the possible symmetry elements (2-fold rotation axis, 2_1 screw axis, mirror plane, *c*-axial or *n*-diagonal glide planes) associated with the *b*-axis only. For orthorhombic symmetry, these symmetry elements may be associated with all three axes. However, while deciphering the possible twin law, we do not need to consider all of the given symmetry elements. The translational parts of the screw axes and glide planes would give rise to systematic absences in reciprocal space, and would therefore give rise to the inclusion of extra symmetry elements rather than the possibility for a crystal twin. Therefore, we only need to consider rotation, reflection and inversion. When we only consider centrosymmetric structures, we will end up with only having to consider 2-fold rotation and mirror operations related to the *a*- and *c*-axes. Mathematically, this means that there are four possibilities: a mirror perpendicular to the *a*-axis, a 2-fold rotation around the *a*-axis, a mirror perpendicular to the *c*-axis and a 2-fold rotation around the *c*-axis, that are described in matrices (i), (ii), (iii) and (iv), respectively. Figure 2.1 shows how the twin domains are related. The blue cells represent twin fraction 1 (h_1,k_1,l_1), the red cell represents twin fraction 2 (h_2,k_2,l_2). For clarity, the cells are projected on the *ab*-plane. The *c*-axis is drawn out-of-plane, and the dashed lines represent the projection on the *ab*-plane with a negative *c*-axis.

$$\begin{bmatrix} h_2 \\ k_2 \\ l_2 \end{bmatrix} = \begin{bmatrix} -1 & 0 & 0 \\ 0 & 1 & 0 \\ 0 & 0 & 1 \end{bmatrix} \begin{bmatrix} h_1 \\ k_1 \\ l_1 \end{bmatrix} \qquad \begin{bmatrix} h_2 \\ k_2 \\ l_2 \end{bmatrix} = \begin{bmatrix} 1 & 0 & 0 \\ 0 & -1 & 0 \\ 0 & 0 & -1 \end{bmatrix} \begin{bmatrix} h_1 \\ k_1 \\ l_1 \end{bmatrix}$$

$$(i) \qquad\qquad (ii)$$

$$\begin{bmatrix} h_2 \\ k_2 \\ l_2 \end{bmatrix} = \begin{bmatrix} 1 & 0 & 0 \\ 0 & 1 & 0 \\ 0 & 0 & -1 \end{bmatrix} \begin{bmatrix} h_1 \\ k_1 \\ l_1 \end{bmatrix} \qquad \begin{bmatrix} h_2 \\ k_2 \\ l_2 \end{bmatrix} = \begin{bmatrix} -1 & 0 & 0 \\ 0 & -1 & 0 \\ 0 & 0 & 1 \end{bmatrix} \begin{bmatrix} h_1 \\ k_1 \\ l_1 \end{bmatrix}$$

$$(iii) \qquad\qquad (iv)$$

In the centrosymmetric case we describe here, we see that (i) and (ii) describe the same cell. This can be seen in Figure 2.1, where both (i) and (ii) cells are related by an inversion operation. Furthermore, this can be seen in the matrices, where an inversion matrix relates both transformation matrices. The same argument holds for (iii) and (iv). Moreover, since monoclinic symmetry has either *m*, 2 or $2/m$ point symmetry associated with the *b*-axis, the *b*-axis can flip in sign (mirror perpendicular to *b*) and describe the same cell. As a result, (i) and (iv), and (ii) and (iii) describe the same cell. Therefore, when any of the four matrices is applied, the same twin will be created. Note that this twinning can indeed only occur when $\beta \approx 90°$, otherwise the inversion of the *b*-axis will not provide the same cell. For the refinement, it does not matter which of the twin matrices is applied to the data, as they are equivalent in reciprocal space. However, either

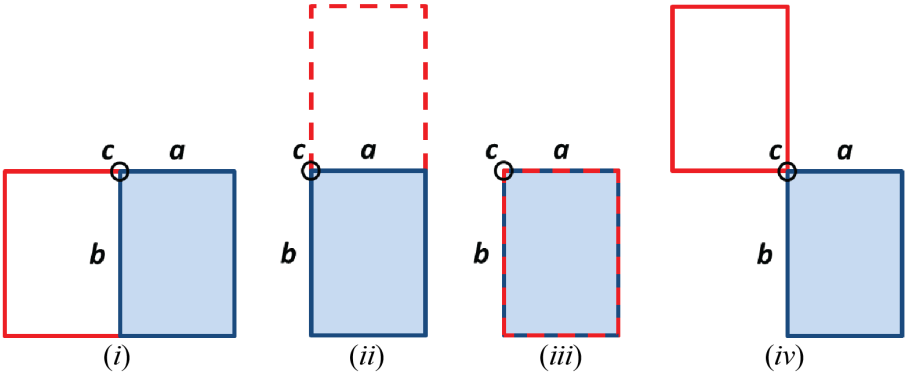

Figure 2.1: *Schematic illustration of symmetry operations that allow the formation of twin domains in monoclinic unit cells that emulate orthorhombic.* (i), (ii), (iii) *and* (iv) *correspond to a mirror perpendicular to the a-axis, a 2-fold rotation around the a-axis, a mirror perpendicular to the c-axis and a 2-fold rotation around the c-axis, respectively. For clarity, the cells are projected on the ab-plane. The c-axis is drawn out-of-plane, and the dashed lines represent the projection on the ab-plane with a negative c-axis.*

of the two twin laws describing the rotation around an axis ((ii) and (iv)) has to be used in the software, as the other two matrices change the handedness of the axes and give a determinant of -1, which is not accepted.

Monoclinic unit cells with a and c approximately equal and $\beta \approx 120°$ may emulate hexagonal. Due to the convention for monoclinic symmetry (the b-axis unique), the monoclinic cell mimics a hexagonal cell where the axes are defined in nonconventional settings, *i.e.* the b-axis is the unique axis, rather than the c-axis. As hexagonal symmetry always has rotational symmetry operators around the c-axis, this means that in our mimicking monoclinic cell, we can have twin fractions that are related by rotation around its b-axis. As here, $\beta \approx 120°$, we can obtain a twin fraction (h_2, k_2, l_2) from the original cell (h_1, k_1, l_1) by 120° rotation around the b-axis, as shown in the left matrix. However, this allows for the presence of a third twin fraction (h_3, k_3, l_3), rotated from the twin fraction 2 by 120° rotation around the b-axis, as shown in the right matrix. As a result, this gives rise to three twin fractions that are related by a 3-fold rotation around the b-axis.

$$\begin{bmatrix} h_2 \\ k_2 \\ l_2 \end{bmatrix} = \begin{bmatrix} 0 & 0 & 1 \\ 0 & 1 & 0 \\ -1 & 0 & -1 \end{bmatrix} \begin{bmatrix} h_1 \\ k_1 \\ l_1 \end{bmatrix} \qquad \begin{bmatrix} h_3 \\ k_3 \\ l_3 \end{bmatrix} = \begin{bmatrix} 0 & 0 & 1 \\ 0 & 1 & 0 \\ -1 & 0 & -1 \end{bmatrix} \begin{bmatrix} h_2 \\ k_2 \\ l_2 \end{bmatrix}$$

Twinning by Reticular Pseudo-Merohedry

Rhombohedral unit cells can have twinning by reticular pseudo-merohedry, when described by hexagonal axes. The hexagonal crystal family consists of two lattice

systems: hexagonal and rhombohedral. These two lattice systems describe unit cells with $a = b$, $\alpha = \beta = 90°$ and $\gamma = 120°$, and $a = b = c$ and $\alpha = \beta = \gamma \neq 90°$, respectively. While the hexagonal symmetry always allows for a 6-fold rotation axis (holohedral point group $6/mmm$), the rhombohedral lattice always has a 3-fold rotation axis (holohedral point group $\bar{3}m$). However, the conventional cell for the rhombohedral lattice is the rhombohedrally-centered (R-centered) hexagonal cell. This cell contains three lattice points and is therefore non-primitive. Still, the choice of this setting can be favored as the 90° angles allow for a coordinate system that is easier to deal with. It is also possible to describe a hexagonal cell in a rhombohedral lattice, but this is rarely favorable. When a rhombohedral cell is described with hexagonal axes, it can mimic the 6-fold rotation symmetry operation present in hexagonal cells by twinning with an additional 2-fold rotation operator parallel to the 3-fold axis. Note that this is not twinning by merohedry, because the 6-fold rotation axis belongs to the $6/mmm$ Laue group, which does not belong to the rhombohedral crystal system. Instead, it is referred to as obversereverse twinning or twinning by reticular pseudo-merohedry. This means that the a- and b-axis can be inverted, in order to mimic the 6-fold rotation. This twinning is described by the matrix below.

$$\begin{bmatrix} h_2 \\ k_2 \\ l_2 \end{bmatrix} = \begin{bmatrix} -1 & 0 & 0 \\ 0 & -1 & 0 \\ 0 & 0 & 1 \end{bmatrix} \begin{bmatrix} h_1 \\ k_1 \\ l_1 \end{bmatrix}$$

Twinning by Non-Merohedry

As described in the previous paragraph, twinning by merohedry, pseudo-merohedry and reticular merohedry are represented by twin matrices that only contain the values 0, 1 and -1. This means that all Miller indices are converted into other integer indices, so that all reciprocal lattice points overlap, even though reflections from one domain may overlap with systematic absences from another. This does not have to be the case. When only a certain set of reciprocal lattice points overlap, while others do not, we speak of twinning by non-merohedry. This means that only reflections with certain Miller indices are affected by the twin law. As a result, the diffraction pattern is a superposition of three sets of reflections: reflections that are present in both twin domains and reflections that are present in either of the two twin domains. Of course, this is not limited to only two twin domains.

A twin law for twinning by non-merohedry often describes a symmetry operation that belongs to a higher symmetry supercell. However, this is not always the case. It is not always possible to describe the relation between the twin fractions by a twin law that belongs to any crystal system or metric symmetry. Such an example is two twin domains rotated by only 15°. In that case, the CELL_NOW[10] software can be used to determine the two independent orientation matrices needed to describe the twin fractions. This is done prior to the integration of the data. In CELL_NOW, we input a full set of reflections and specify the unit cell parameter (or let CELL_NOW search for the best fitting cell within given margins). CELL_NOW outputs the amount of reflections that have an integer index in the specified cell and gives the amount of unindexed reflections. Searching for

the next twin domain, CELL_NOW rotates the unit cell in such a way that fits again, and outputs the total number of indexed reflections in the second domain, the number of reflections that are unique for the second domain and the amount of reflections that are not yet assigned to any domain. Furthermore, the transformation matrix with respect to the first twin domain is given. This process can be continued until (almost) all reflections are assigned to a twin domain. Once finished, both HKL4 and HKL5 reflection data files can be created. Usually, all reflections are listed in an HKL4 file, listing h, k, l, F^2 and $\sigma(F^2)$. When twinning by non-merohedry occurs, each reflection that corresponds to an overlap or partial overlap of the two twin domains should appear twice (or more in case of more twins) in the HKL4 file. Since this is not possible, the HKL5 file is generated as well. In addition to the HKL4 file, it lists which transformation matrix should be applied to each reflection, *i.e.* to which domain each reflection is assigned to. The integration should then be done over all twin domains using the HKL5 file, followed by an absorption correction including all twin domains, using TWINABS.[19] With the generated HKL4 file, the structure solution can be determined. Introducing the HKL5 file during the refinement, with corresponding weighting fractions, should greatly enhance the overall fit of the structure solution. Refinement of the weighting fractions will indicate the individual sizes of the domains.

The Combination of Multiple Twins

It is possible that a crystal has multiple twin domains. I have shown this in the example of the monoclinic unit cell with a and c approximately equal and $\beta \approx 120°$, which has three twin domains. I have also shown that twinning by non-merohedry is not restricted to two twin domains, and even a lot more domains can be present. In Chapter 5 I describe a crystal that consists of twelve twin domains. It is also possible that more than one *twin law* is needed to describe all twin domains. This is relatively easy for the combination of general and racemic twins. For example, a monoclinic unit cell with $\beta \approx 90°$ and space group $P2_1$ can have twinning by pseudo-merohedry as well as racemic twinning due to the fact that $P2_1$ is a non-centrosymmetric space group. As a result, the inversion matrix can be applied to either of the two domains related by the first twin, resulting in a total of four twin domains. The combination of twinning by (pseudo-)merohedry and racemic twinning can be included in SHELX97, using an HKL4 file and the following command in the refinement:

$$\text{TWIN } -1\,0\,0\;\; 0\,-1\,0\;\; 0\,0\,-1\;\; -4$$

Here, the twin operation of matrix (iv) is given. Addition of the '4' gives a total of four twin domains, and the '$-$' makes sure that racemic twinning is included. Furthermore, four weighting fractions should be refined as well.

It is not possible to add a TWIN command to refine an HKL5 file. However, racemic twinning can also be included in CELL_NOW, to create twice as many twin domains in the HKL5 file. CELL_NOW can also be used to combine twinning by (pseudo-)merohedry and non-merohedry. For example, consider a monoclinic cell with $\beta \approx 90°$ and $a \approx 2b$. This β angle allows for twinning by pseudo-merohedry and $a \approx 2b$ allows for twinning around the c-axis by 90°. This second twin is caused by non-merohedry as it mimics a tetragonal cell when the a-axis is doubled. As a result, a 4-fold axis around the c-axis can

be present. In order to rotate the second domain by 90° from the first domain, the twin matrix below should be applied.

$$\begin{bmatrix} h_2 \\ k_2 \\ l_2 \end{bmatrix} = \begin{bmatrix} 0 & 2 & 0 \\ -0.5 & 0 & 0 \\ 0 & 0 & 1 \end{bmatrix} \begin{bmatrix} h_1 \\ k_1 \\ l_1 \end{bmatrix}$$

Only the data with $h = 2n$ are affected by this twin, by showing overlap of the diffraction patterns. As this twin is by non-merohedry, it can be found by CELL_NOW. The twinning by pseudo-merohedry will not be suggested, as addition of this twin does not give more indexing of the reflections. After all, this is twinning by pseudo-merohedry, so all reflections overlap. Manually applying the twin matrix to both cells found by CELL_NOW allows for inclusion of all four twin domains, and in case of a non-centrosymmetric space group, racemic twinning can give a total of eight twin domains. Refinement of the HKL5 file with eight weighting fractions can give the final solution.

2.4 Conclusions

In conclusion, I have highlighted various experimental strategies that play a major role in all research projects described in the following chapters. These experimental strategies include the synthesis methods, patterning techniques and X-ray diffraction data interpretation I have conducted in this thesis.

The synthesis of various organic-inorganic hybrid materials is one of the key aspects of the research projects described in the following chapters. Here, I have provided an overview of all synthesis methods carried out in this thesis. These methods include the synthesis of the organic precursors salts, crystal growth from slow evaporation, the layered-solution crystal-growth technique and crystal growth of air-sensitive compounds. I have explained how the preferred synthesis method depends on various factors, including solubility and air-sensitivity of the precursors and end-product. Moreover, I have described the advantages and disadvantages of each method. My findings are that there is no chemical preference for using a pre-made organic precursor salts over the liquid precursor, despite the fact that the organic precursor salt can be easier to handle. Furthermore, synthesis methods based on slow evaporation are relatively easy, but not applicable to poorly soluble inorganic precursors. On the other hand, the layered-solution crystal growth technique works well for inorganic precursors that have a generally poor solubility, but does not work for compounds that tend to dissolve in water and ethanol. In addition to these synthesis techniques, I also described how to deal with air-sensitive compounds and how to pattern polycrystalline microstructures.

Structure determination by XRD plays a major role in all research carried out in this thesis, because understanding structure-property relations in organic-inorganic hybrid materials is the main goal in each chapter. I have highlighted some of the key aspects of XRD that I have taken into consideration when solving the crystal structures. These include, but are not limited to, measuring a full limiting sphere, refinement in triclinic settings, the use of non-standard space group settings and incorporation of crystal twinning. Moreover, I have highlighted the benefits of using powder XRD as a complementary method. Note that other experimental techniques carried out by me or collaborations are described in the experimental sections of each of the following chapters.

Bibliography

[1] Baikie, T.; Fang, Y.; Kadro, J. M.; Schreyer, M.; Wei, F.; Mhaisalkar, S. G.; Graetzel, M.; White, T. J. *J. Mater. Chem. A* **2013**, *1*, 5628–5641.

[2] Liu, J.; Xue, Y.; Wang, Z.; Xu, Z.-Q.; Zheng, C.; Weber, B.; Song, J.; Wang, Y.; Lu, Y.; Zhang, Y.; Bao, Q. **2016**,

[3] Fang, H.-H.; Raissa, R.; Abdu-Aguye, M.; Adjokatse, S.; Blake, G. R.; Even, J.; Loi, M. A. *Adv. Funct. Mater.* **2015**, *25*, 2378–2385.

[4] Huang, T. J.; Thiang, Z. X.; Yin, X.; Tang, C.; Qi, G.; Gong, H. *Chem. Eur. J.* **2016**, *22*, 2146–2152.

[5] Arkenbout, A. *PhD Thesis* **2010**, University of Groningen.

[6] Polyakov, A. O. *PhD Thesis* **2014**, University of Groningen.

[7] Mitzi, D. B. *J. Solid State Chem.* **1999**, *704*, 694–704.

[8] Stoumpos, C. C.; Malliakas, C. D.; Kanatzidis, M. G. *Inorg. Chem.* **2013**, *52*, 9019–9038.

[9] Ten Elshof, J. E.; Khan, S. U.; Göbel, O. F. *J. Eur. Ceram. Soc.* **2010**, *30*, 1555–1577.

[10] Sheldrick, G. M. *CELL_NOW*; University of Göttingen: Göttingen, **2008**.

[11] Cockcroft, J. K. *A Hypertext Book of Crystallographic Space Group Diagrams and Tables*; Birkbeck College, University of London: `http://img.chem.ucl.ac.uk/sgp/mainmenu.htm`.

[12] De Wolff, P. M.; Billiet, Y.; Donnay, J. D. H.; Fischer, W.; Galiulin, R. B.; Glazer, A. M.; Hahn, T.; Senechal, M.; Shoemaker, D. P.; Wondratschek, H.; Wilson, A. J. C.; Abrahams, S. C. *Acta Cryst.* **1992**, *A48*, 727–732.

[13] Parsons, S. *Acta Cryst.* **2003**, *D59*, 1995–2003.

[14] Friedel, G. *Leçons de Cristallographie*; Berger-Levrault: Paris, **1928**.

[15] Sheldrick, G. M. *SHELX97, Program for Crystal Structure Refinement*; University of Göttingen: Göttingen, **1997**.

[16] Flack, H. D. *Acta Cryst.* **1983**, *A39*, 876–881.

[17] Hahn (Ed.), T. *International Tables for Crystallography. Vollume A: Space-Group Symmetry*; Springer: Netherlands, **2002**.

[18] Parkin, S. *Tutorial: Twinning by Pseudo-Merohedry in SHELXL*; University of Kentucky: `http://xray.uky.edu/Tutorials/pseudo-merohedry/pseudo-merohedry_0.html`, **2011**.

[19] Sheldrick, G. M. *TWINABS*; University of Göttingen: Göttingen, **2012**.